A model-based investigation of tool-chip friction during precision micro cutting of commercially pure titanium alloy

Alp Aksin

Department of Mechanical Engineering,
Bilkent University,
Ankara, 06800, Turkey
Email: alp.aksin@bilkent.edu.tr

Yiğit Karpat*

Department of Industrial Engineering,
Bilkent University,
Ankara, 06800, Turkey

and

Department of Mechanical Engineering,
Bilkent University,
Ankara, 06800, Turkey

and

UNAM – Institute of Materials Science and Nanotechnology,
Ankara, 06800, Turkey
Fax: +90 312 266 4054
Email: ykarpat@bilkent.edu.tr
*Corresponding author

Abstract: Understanding interaction between the cutting tool edge radius and the work material is essential to identify the conditions leading to superior surface finish during the micromachining process. The interaction between friction angle and effective rake angle has been investigated based on a slip-line field-based machining model from the literature. Machining forces and cut chip thickness values were obtained from orthogonal cutting tests and employed in the process model. The proposed model also allows for calculating material properties such as shear flow stress and fracture toughness. The proposed model can successfully simulate machining forces during shearing-dominated machining conditions. The results showed the importance of flank and rake face friction in micro-scale machining.

Keywords: micro cutting; edge radius; friction; ductile fracture; machining; slip line field.

Reference to this paper should be made as follows: Aksin, A. and Karpat, Y. (xxxx) 'A model-based investigation of tool-chip friction during precision micro cutting of commercially pure titanium alloy', *Int. J. Mechatronics and Manufacturing Systems*, Vol. x, No. x, pp.xxx–xxx.

Biographical notes: Alp Aksin received his BS degree from Dokus Eylul University and MSc degree from Bilkent University, Department of Mechanical Engineering and currently working at Roketsan.

Yiğit Karpat is an Associate Professor of Bilkent University Industrial Engineering Department. He is also affiliated with Bilkent Mechanical Engineering and UNAM. His research interest is precision machining.

1 Introduction

Metal cutting theory mainly considers energy spent on shearing and friction in the cutting zone (Backer et al., 1952). While there is a consensus about the energy required to create a new surface during machining, whether it is negligible or not is an ongoing debate. Atkins (2003) pointed out that in finite element modelling of machining processes, a separation criterion is implemented to simulate chip formation. However, it is omitted in analytical machining models. According to Atkins, shear flow stress and fracture toughness of the material must be included in machining models since both would provide a better definition of the material behaviour during deformation. Atkins calculated the work necessary for new surface creation to be in the range of kJ/m^2 at macro-scale machining conditions. He concluded that not considering the fracture toughness leads to high shear flow stress values at low uncut chip thickness values. He related the fracture toughness to the positive intercept of forces at zero chip thickness which are interpolated from large chip thickness values. In his analysis, Atkins neglected the effect of cutting edge radius on the forces. Karpat (2009) investigated the interaction between edge radius and fracture toughness. He utilised a slip-line field model with a stagnant metal zone (or dead metal zone) in front of the tool edge adapted from a previous study (Karpat and Özel, 2008). He proposed a method to calculate fracture toughness as a function of uncut chip thickness. The fracture toughness of the material was calculated to be smaller when the cutting edge is considered. Subbiah and Melkote (2007) provided experimental evidence by investigating the fractured regions at the chip roots through quick stop tests. They showed that the edge radius of the cutting tool creates the necessary conditions to initiate fracture during the chip formation process. Parle et al. (2016) also evaluated fracture energy of micro cutting of ductile materials by using J-integral approach. They concluded that the contribution of fracture term to the size effect is in the range of 4–24% for various conditions. In a recent study, Zheng et al. (2021) investigated the influence of using surface-active medium on the machinability of maraging steel where the model of Karpat (2009) was extended to including the elastic contact on the flank face of the tool. They integrated the calculated fracture toughness into the finite element model to simulate the positive influence of applying surface-active medium on the process outputs.

On the other hand, Childs (2010) used finite element simulations of machining, without including any fracture model, to show that the edge radius and its interaction with material properties are responsible for the size effect. He concluded that there is no need to include fracture toughness in the models. He also pointed out that the fracture toughness (kJ/m^2) is equivalent to edge forces (N/mm) due to the ploughing action of the cutting edge radius. He commented that increasing shear flow stress with decreasing temperature and increasing strain rate at low uncut chip thickness explains the size effect. The influence of the work material is represented with material constitutive models. Melkote et al. (2017) have shown the close relationship between the material constitutive and friction models within the framework of the machining process. Recently, Feng and Sagapuram (2021) have shown that rake face friction can be used to explain the size effect based on their experiments with glass edge knives in the absence of edge radius. Karpat (2022) conducted plunging type orthogonal machining experiments on commercially pure titanium with diamond cutting tools. The adhesion between the work material and the tool on the flank face was shown to contribute to the size effect significantly. When tool edge radius is considered, such a relationship becomes more complex. A better understanding of friction conditions would lead to improved designs of micro textured cutting tools are reported in Patel et al. (2019) and tailored micro end mill designs reported in Oliaei and Karpat (2019).

The contact conditions between the cutting edge and the work material affect the material flow around the cutting zone during micro-scale machining. When uncut chip thickness is less than the edge radius, the effective rake angle determines the material flow, which directly affects the friction conditions. In this study, an experimental study on micro-scale machining of commercially pure titanium has been conducted. Machining forces and cut chip thickness values were measured experimentally. An iterative methodology has been proposed to calculate the material properties and internal process parameters iteratively, and the interplay between shearing, friction, and surface energy is investigated during titanium alloy micro-scale machining.

2 Modelling and solution methodology

Contributions of shearing, friction (rubbing and ploughing), and new surface formation work can be written as in Eq.1 for the slip-line model presented in Figure 1(a) (Karpat, 2009). In this model, a stagnant material zone (SMZ) is assumed to exist in front of the cutting edge (Karpat and Özel, 2008).

$$F_c V = \frac{\tau_y h w \cos(\alpha) V}{\sin(\phi)\cos(\phi-\alpha)} + \frac{F_r \sin(\phi) V}{\cos(\phi-\alpha)} + \frac{F_p \sin(\xi_1-\lambda) V}{\xi_1} + R w V \tag{1}$$

In equation (1), τ_y is the shear yield stress, R is the fracture toughness (specific work of surface formation), h is the uncut chip thickness, w is the width of cut, V is the cutting speed, α is the effective tool rake angle, ϕ is the shear angle of the primary shear zone, F_r is the rubbing force at secondary shear zone, F_p is the ploughing force under the

stagnant metal zone, ξ_1 is the slip-line angle and lastly λ is the inclination angle of the stagnant metal zone. In this study, the effective rake angle α given in equation (1) and shown in Figure 1(b) is considered as an unknown variable. Due to edge radius, effective rake angle is assumed to be changing with respect to uncut chip thickness.

Figure 1 (a) illustration of slip-line field model (Karpat and Özel, 2009) and (b) rubbing and ploughing force component at SMZ

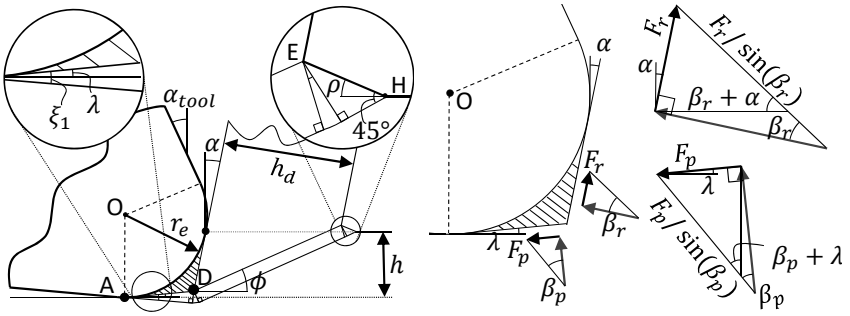

(a) (b)

Slip-line angle ξ_1 can be calculated (Fang, 2003) as $\xi_1 = arccos(m)/2$, where, *m*, is the friction factor under stagnant metal zone (boundary $|AD|$ in Figure 1(a)). Friction factor is defined as $m = \tau_y / k$ in which k is the shear flow stress which is constant with the assumption of perfectly plastic work material with no strain hardening. According to Figure 1(b), cutting force F_c can be written from the force balance as

$$F_c = F_r \frac{\cos(\beta_r - \alpha)}{\sin(\beta_r)} + F_p \frac{\sin(\beta_p + \lambda)}{\sin(\beta_p)} \tag{2}$$

where, β_r is the friction angle for rubbing force and β_p is the friction angle for ploughing force. Ploughing force is evaluated under stagnant metal zone as

$$F_p = m\tau_y |AD| w \tag{3}$$

Rubbing force can be calculated as function of F_c by substituting equation (3) to equation (2) then writing for F_r:

$$F_r = \frac{F_c \sin(\beta_r)}{\cos(\beta_r - \alpha)} - \frac{m\tau_y |AD| w \sin(\beta_p + \lambda)\sin(\beta_r)}{\cos(\beta_r - \alpha)\sin(\beta_p)} \tag{4}$$

In equation (4), the length of $|AD|$ is given as (see Figure 3(a))

$$|AD| = \frac{r_e[1+\sin(\alpha)]}{\cos(\lambda - \alpha)} \tag{5}$$

where, r_e is the edge radius of the cutting tool. In addition, calculation of β_p and prow angle ρ is given in (Karpat and Özel, 2009). Substituting equations (4), (3) into equation (2) yields equation (6). The terms, N and Q are defined in equations (7) and (8), respectively.

$$F_c = \frac{\tau_y h w \cos(\alpha)}{\sin(\phi)\cos(\phi-\alpha)Q} - \frac{m\tau_y \mid AD \mid w}{Q} N + \frac{Rw}{Q} \tag{6}$$

$$N = \left[\frac{\sin(\xi_1 - \lambda)}{\xi_1} - \frac{\sin(\beta_r)\sin(\phi)\sin(\beta_p + \lambda)}{\cos(\phi-\alpha)\cos(\beta_r - \alpha)\sin(\beta_p)} \right] \tag{7}$$

$$Q = \left[1 - \frac{\sin(\phi)\sin(\beta_r)}{\cos(\phi-\alpha)\cos(\beta_r - \alpha)} \right] \tag{8}$$

Finding shear angle and rubbing angle is the starting point of the solution methodology. To calculate shear angle, minimum energy principle can be used by taking derivative of cutting force (equation (6)) with respect to shear angle which yields equation (9).

$$\begin{aligned} 0 = {} & \frac{\sin(\beta_r)}{\cos(\beta_r - \alpha)} \left[\gamma + \frac{m r_e (1+\sin(\alpha))}{h\cos(\lambda-\alpha)} N + Z \right] - \dots \\ & Q \left[\frac{\cos(2\phi-\alpha)}{\sin^2(\phi)} + \frac{m r_e (1+\sin(\alpha))\sin(\beta_p+\lambda)\sin(\beta_r)}{h\cos(\lambda-\alpha)\sin(\beta_p)\cos(\beta_r-\alpha)} \right] \end{aligned} \tag{9}$$

where Z is the dimensionless parameter and defined in Atkins' model as $Z = R/(\tau_y h)$. In the solution procedure, equation (6) is used for finding β_r rather than ϕ which is the main difference introduced in this study compared to previous work of Atkins (2003) and Karpat (2009). Since uncut chip thickness and cut chip thickness are measured experimentally, direct calculation of ϕ is possible based on a sharp corner assumption which can be justified with the consideration of stagnant material zone in front of the tool. Therefore, shear angle ϕ is assumed to be known for each given uncut and cut chip thickness (h, h_d) pairs, which allows for calculating effective rake angle. The solution algorithm is given in Figure 2, which finds the shear flow stress τ_y, and fracture toughness R using an iterative approach.

In this algorithm, for each (h, h_d) pair ρ, β_p, α and ϕ are calculated. Then, slope (S) and intercept I of cutting force data is found. A vector of possible Z values is created. For each element in Z vector, possible values of β_r, shear strain γ ($\cos\alpha/(\sin\phi\cos(\phi-\alpha))$), Q, N, $|AD|$ are found. Using these, possible values of shear stress are found as $\tau_y = SQ/(w\gamma)$. Subsequently, possible values of fracture toughness are calculated from: $R_I = IQ/w - m\tau_y \mid AD \mid N$.

3 Experimental tests

Micro-scale orthogonal cutting tests were conducted using an ultra-precision turning machine (Moore Nanotech FG350) at the conditions given in Table 1. The experimental

setup is shown in Figure 3(a) and (b). Cutting forces are measured by a dynamometer (Kistler mini dynamometer 9256C1 with a charge amplifier) and recorded by a data acquisition card (NI 7854R A/D converter) with a sampling rate of 333 kHz. Figure 3(c) shows the micro-cutting edge of the grooving tool used in the experiments (Tungalloy). A new cutting edge was used in orthogonal cutting tests. The cutting edge was investigated with a laser topology microscope (Keyence VKX-100) to have edge radii around 2.5 and a rake angle of 20 degrees, as shown in Figure 3(d). Cut (deformed) chip thickness values were measured by using a scanning electron microscope (SEM). Figure 4 shows the SEM image of the cut chip thickness. An average cut chip thickness value was calculated based on multiple measurements taken from different locations. Figure 5 shows the microstructure of the commercially pure titanium used in this study. The material was received in its extruded form. The acicular grain morphology of the material is due to previous work applied to it. The material has HV 200 (or around 1.9 GPa) micro-Vickers hardness.

Figure 2 Flowchart of the solution methodology

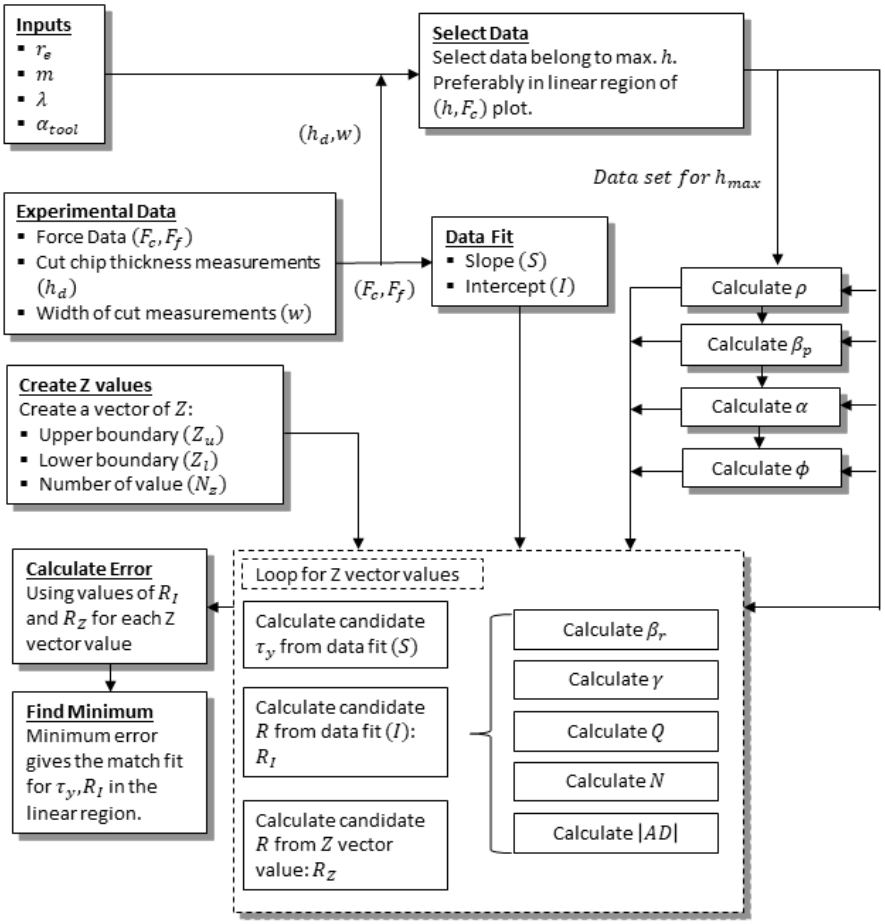

Figure 3 (a, b) Micro orthogonal cutting test setup; (c) image the micro grooving tool and (d) SEM image of unused cutting edge (see online version for colours)

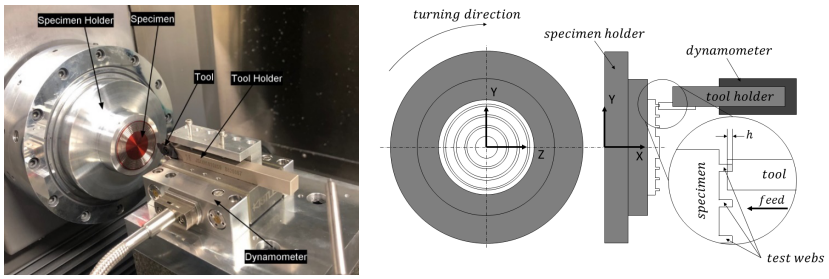

(a) (b)

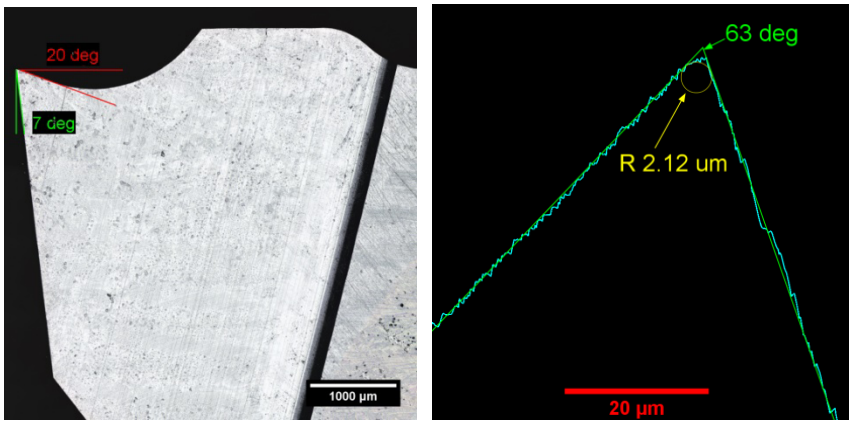

(c) (d)

Figure 4 SEM image of a continuous chip (see online version for colours)

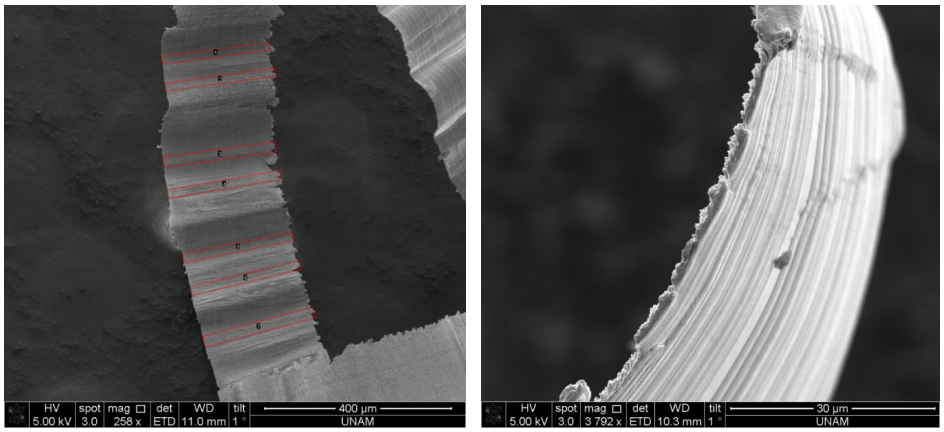

Figure 5 Microstructure of the commercially pure titanium with acicular grains (see online version for colours)

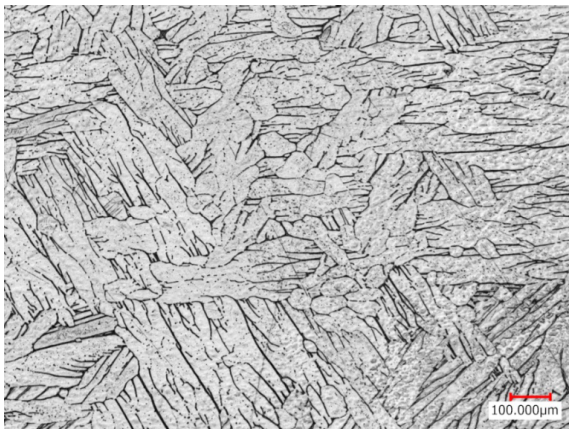

Table 1 Summary of experimental conditions

Parameters	*Values and comments*
Material	CP Ti Grade 2
Cutting speed [m/min]	40
Uncut chip thickness [µm]	0.25, 0.5, 1, 2, 3, 4, 5, 6
Width of cut [µm]	250
Tool	Tungaloy JXPG06R10F SH725
Tool rake angle [°]	20
Tool clearance angle [°]	7
Tool edge radius [µm]	2.5
Tool width [µm]	1000

4 Results

Figure 6(a) shows the measured cutting and thrust forces for different uncut chip thickness values. As expected, cutting forces decrease with decreasing uncut chip thickness. Between 1 µm and 6 µm uncut chip thickness, cutting force measurements present a linear trend Around 1.5 µm uncut chip thickness, feed force measurements become larger than cutting forces, indicating a transition from shearing dominated to ploughing dominated machining region. At uncut chip thicknesses lower than 1 µm, which is around half of the edge radius, the trends in cutting and feed forces start to deviate from the linear trend. The microstructure of the work material and stagnant material zone are important factors affecting the chip formation. Figure 6(b) and (c) shows the cut chip thickness measurements and chip ratio for different test cases. At small uncut chip thickness values, there is a significant increase in cut chip thickness values and hence chip ratio.

Figure 6 (a) Variation of cutting and feed forces as a function of uncut chip thickness; (b) average cut chip thickness measurements as a function of uncut chip thickness and (c) chip ratio calculation based on cut chip thickness data (see online version for colours)

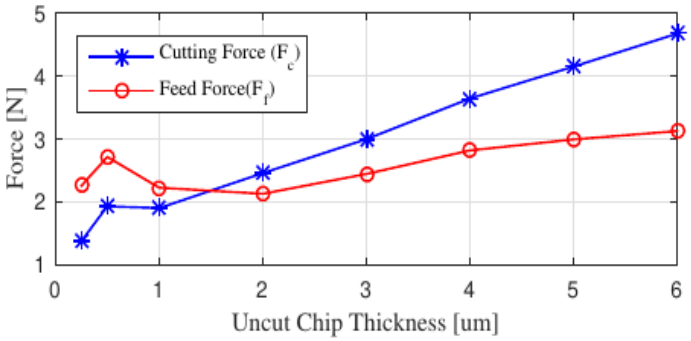

(a)

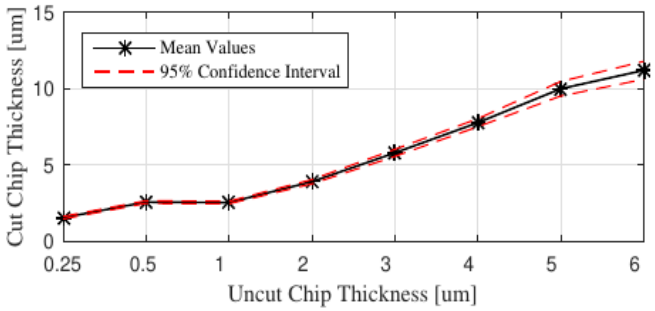

(b)

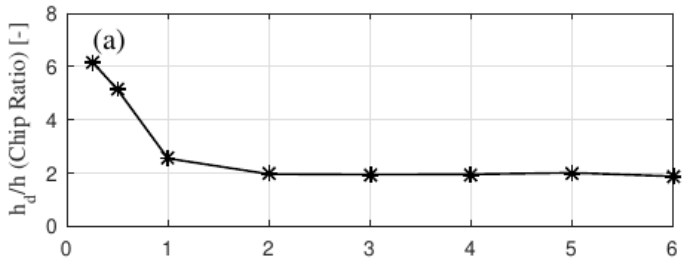

(c)

The experimental data shown in Figure 6 was used to calculate the unknown internal process parameters as explained in Figure 2. The shear flow stress τ_y was calculated as 636 MPa and fracture toughness R was calculated as 3.17 $\mathrm{kJ/m^2}$ for known values of $r_e = 2.5$ µm, $m = 0.94$, $\lambda = 1.5^\circ$. Here, values of m and λ are adapted from literature (Karpat and Özel, 2008). These values are calculated for linear data between 1 µm and 6 µm uncut chip thickness. Table 2 shows the variation of calculated internal parameters as a function of uncut chip thickness based on the model solution. According to Table 2, starting from uncut chip thickness of 1 µm, the effective rake angle values was calculated to be negative and becomes even more negative with decreasing uncut chip thickness. It must be noted that the shear angle values were measured experimentally. The friction

angle β_r decreases with decreasing uncut chip thickness which implies decreasing coefficient of friction, which is the opposite of expected. At large uncut chip thickness, both effective rake angle and coefficient of friction have steady values.

Table 2 Calculated model parameters and specific cutting pressure for uncut chip values for variable effective rake angle assumption

Variable α (*changes with respect to* r_e *and* h)					
h	Z	ϕ	β_r	α	F_c/wh
[μm]	[–]	[deg]	[deg]	[deg]	[N/m^2]
0.25	19.9	5.1	14.2	–61	28,052
0.50	10	9.5	15.8	–-48.7	14,733
1	4.85	16.6	19.5	–29	7946
2	2.44	25.3	28.2	0	4734
4	1.22	27.2	29	0	3504
6	0.80	27.9	29.6	0	3078

Figure 7 shows the simulated forces based on the calculated values shown in Table 2. Cutting and feed forces are predicted with error of 2.76% and 10.92%, respectively. The feed force predictions do not agree well with the measurements at uncut chip thicknesses less than 1 μm. The model is not capable of capturing the variations in the feed forces at ploughing dominated region.

Figure 7 Model predictions based on calculated parameters under variable effective rake angle assumption

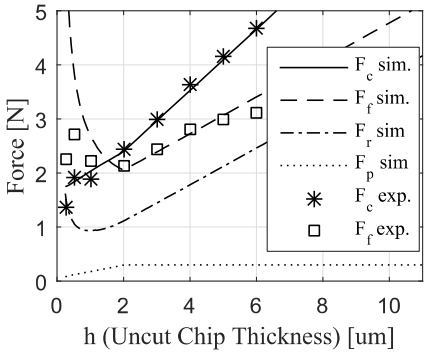

To check the influence of effective rake angle on the results, it is assumed that a zero rake angle is constant for all test cases. The results are recalculated by using the same methodology. The results are shown in Table 3. In this case, the shear flow stress τ_y and fracture toughness R are calculated as 644 MPa and 3.18 $\frac{\text{kJ}}{\text{m}^2}$, which are quite close to the previously calculated values. With decreasing uncut chip thickness, coefficient of friction increases which matches with experimental observations of coefficient of friction.

Table 3 Calculated model parameters and specific cutting pressure for uncut chip values under zero effective rake angle assumption

Constant $\alpha = 0°$					
h	Z	ϕ	β_r	α	F_c/wh
0.25	19.75	9.52	49.11	0	24520
0.50	9.93	14.64	39.26	0	13392
1	4.80	20.16	33.15	0	7600
2	2.41	24.35	30.40	0	4903
4	1.21	27.13	29.29	0	3547
6	0.80	28.23	29.02	0	3077

Figure 8 shows the cutting and feed force predictions with errors decreased to 2.1% and 3.8%, respectively. The feed force predictions are significantly improved, yet the model still cannot capture the jump in forces observed at 0.5 μm uncut chip thickness. It must be noted the calculated friction angle values are based on assumed friction factor and its angle at the stagnant material zone. Therefore, changing the friction factor at the stagnant metal region would lead to a different set of coefficients of friction parameters.

Figure 8 Model predictions based on calculated parameters under constant rake angle assumption

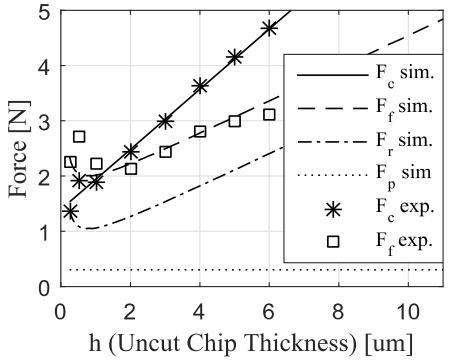

5 Conclusions

The results of this study indicated the importance of correctly identifying friction conditions and its relationship with material properties during micro scale machining. The proposed model can achieve acceptable predictions in shearing dominated region of micro machining and it can also be used to calculate shear flow stress and fracture toughness of the material. The small value of fracture toughness can be attributed to the small edge radius of the cutting tool used in the experiments. The results indicate that fracture toughness alone cannot describe the size effect. Additional research is required to

improve the model predictions in the ploughing dominated region where the material flow around the cutting edge is affected by many different factors simultaneously. Instead of using orthogonal cutting tests, where the tool is constantly fed into the workpiece, plunging type of cutting experiments can be performed. Therefore, variation of forces can be monitored as a function of tool movement which can be beneficial to better understand the interaction between the cutting edge radius and the material during micro scale machining.

References

Atkins, A.G. (2003) 'Modelling metal cutting using modern ductile fracture mechanics: quantitative explanations for some longstanding problems', *Int. J. Mech. Sci.*, Vol. 45, pp.373–396.

Backer, W.R., Marshall, E.R. and Shaw, M.C. (1952) 'The size effect in metal cutting', *Trans. ASME*, Vol. 74, pp.61–72.

Fang, N. (2003) 'Slip-line modeling of machining with a rounded-edge tool–parts I and II', *Mech. Phys. Solids*, Vol. 51, pp.715–762.

Feng, G. and Sagapuram, D. (2021) 'A strong basis for friction as the origin of size effect in cutting of metals', *International Journal of Machine Tools and Manuf.*, Vol. 168, Part B, 103741.

Karpat, Y. (2022) 'Investigating flank face friction during precision micro cutting of commercially pure titanium via plunging tests with diamond grooving tools', *Journal of Materials Processing Tech*., Vol. 299, p.117376.

Karpat, Y. (2009) 'Investigation of the effect of cutting tool edge radius on material separation due to ductile fracture in machining', *International Journal of Mechanical Sciences*, Vol. 51, pp.541–546.

Karpat, Y. and Özel, T. (2008) 'Mechanics of high speed cutting with curvilinear edge tools', *Int. J. Mach. Tools Manuf.*, Vol. 48, pp.195–208.

Melkote, S.N., Grzesik, W., Outeiro, J., Rech, J., Schulze, V., Attia, H., Arrazola, P.J., M'Saoubi, R. and Saldana, C. (2017) 'Advances in material and friction data for modelling of metal machining', *CIRP Annals – Manufacturing Tech*., Vol. 66, pp.731–754.

Oliaei, S.N.B. and Karpat, Y. (2019) 'Modeling and analysis of tool deflection in tailored micro end mills', *International Journal of Mechatronics and Manufacturing Systems*, Vol. 12-1, pp.20–37.

Parle, D., Singh, R.K. and Joshi, S.S. (2016) 'Fracture energy evaluation using J-internal in orthogonal microcutting', *ASME. J. Micro Nano-Manuf.*, Vol. 4, No. 1, pp.011002–011002–9.

Patel, K., Kaftanoglu, B. and Ozel, T. (2019) 'Micro textured cutting tool effects on cutting forces, volumetric wear and adhesion in dry turning of titanium alloy', *International Journal of Mechatronics and Manufacturing Systems*, Vol. 12, Nos. 3–4, pp.180–195.

Subbiah, S. and Melkote, S.N. (2007) 'Evaluation of Atkins' model of ductile machining including the material separation component', *Journal of Materials Processing Technology*, Vol. 182, pp.398–404.

Childs, T.H.C. (2010) 'Surface energy, cutting edge radius and material flow stress size effects in continuous chip formation of metals', *CIRP Journal of Manufacturing Science and Technology*, Vol. 3, pp.27–39.

Zheng, Z., Jin, Y., Zhang, J.L., Jin, X. and Wang, H. (2021) 'Ultra-precision micro-cutting of maraging steel 3J33C under the influence of a surface-active medium', *Journal of Materials Processing Technology*, Vol. 292, p.117054.

Nomenclature

α	Rake angle	F_r	Rubbing force
β	Friction angle	F_p	Ploughing force
λ	Slip line angle	R	Fracture toughness
ϕ	Shear angle	m	Friction factor
ξ	Slip line angle	k	Shear flow stress at the DMZ
ρ	Prow angle	r_e	Edge radius
γ	Shear strain	Z	Dimensionless parameter
τ_y	Shear flow stress	V	Cutting speed
F_c	Cutting force	h	Uncut chip thickness
F_f	Feed force	w	Width of cut